

Molecular Dynamics Simulation of 4-N-Hexyl-4'-Cyanobiphenyl Adsorbed at the Air-Water Interface

Oğuz Gürbulak, Emine Cebe**

Department of Physics, Faculty of Science, Ege University, Bornova 35100, Izmir, Turkey

(Received 6 November 2017)

The interfacial behavior of 4-*n*-hexyl-4'-cyanobiphenyl (6CB) molecules at the air-water interface is investigated by full atomistic molecular dynamics simulations. To understand the morphology and the structure of adsorbed 6CB molecules in detail, the snapshots and mass density profiles of the simulation system are generated. The average tilt angles between the interface normal and various vectors defined in the rigid and alkyl parts of 6CB are in good agreement with the experimental data available. The interfacial thickness and monolayer width are obtained from the mass density profiles of water and 6CB phase, respectively. The second and fourth rank orientational order parameters of cyanobiphenyl core are found to be larger than those of an elastic alkyl chain. Bond order parameters for 6CB are also calculated. The calculated oxygen-oxygen radial distribution function and hydrogen bonding statistics for bulk water are compared with those for the interfacial region. The surface tensions of the systems are calculated. All simulation results are compared with the available literature data.

PACS: 68.35.Ct, 31.15.xv, 61.30.Gd, 68.03.-g

DOI: 10.1088/0256-307X/35/4/046802

Most technological applications of liquid crystals depend on controlling the molecular orientation at an interface or a surface. This kind of control is accomplished through chemistry, topography and the adsorption of surfactants or monolayers.^[1] Liquid crystalline interfaces occur when liquid crystal (LC) molecules are anchored to a solid surface, the isotropic phase and the nematic phase coexist, or when LCs are encircled by vapor. Interfacial properties of LCs are of practical importance to design optical devices. It is a necessity in many devices to control the molecular tilt and the alignment of liquid crystal molecules is strongly affected by their proximity to interfaces.^[2]

LC molecules are able to form the Langmuir monolayers at the air-water (A/W) interfaces. A Langmuir monolayer is an ideal model system to study the two-dimensional phase behaviors of amphiphilic surfactant and biopolymer molecules in many colloidal and biological systems.^[3] Daniel *et al.* showed that *n*-alkyl-cyanobiphenyl (*n*CB) liquid crystals could be spread as the Langmuir monolayers.^[4] The *n*-alkyl-cyanobiphenyls consist of a polar cyano group, a biphenyl chromophore and an alkyl chain containing *n* methylene/methyl groups. The *n*CB homologous series with *n* = 5–12 are the commonly studied liquid crystals. Remarkable experimental studies on *n*CB Langmuir monolayers have been published.^[5–8] However, the detailed interfacial properties at the molecular level are difficult to distinguish experimentally, because the fraction of interfacial molecules is quite small in comparison with that of the bulk medium. Therefore, the simulation studies on monolayers at the A/W interface are an active area for scientists. A small number of simulation studies on the interfacial properties of only two members of *n*CB series, namely 5CB and 8CB, have been reported.^[9,10] In these studies, united atom models, in which the hydrogen atoms

are ignored, were used. Recently, utilizing the OPLS all-atom (OPLS-AA) model, we performed molecular dynamics simulations for quantifying some interfacial properties of 8CB monolayers on water substrate and we noticed that the simulated data are generally in agreement with experiments.^[11] In the present study, we examine the interfacial properties (i.e., mass density profiles, interfacial thickness, monolayer width, hydrogen-bonding, molecular ordering, tilt angle, surface tension and radial distribution function) of 6CB monolayers at the A/W interface, by performing full atomistic molecular dynamics (MD) simulations. To the best of our knowledge, adsorbed 6CB molecules at the A/W interface have never been studied by full atomistic MD simulations before.

Here 5543 water molecules in a cubic cell were simulated for 40 ns at 297 K in an NpT ensemble. The TIP4P/2005 model was employed for water.^[12] An aqueous phase containing equilibrated water molecules was put in the center of the rectangular box (54.984 Å (*x*) × 54.984 Å (*y*) × 300.000 Å (*z*)). The molecular geometry of 6CB was optimized by a Gaussian 09 electronic structure package^[13] at the B3LYP/6-31G* level of theory. Considering the surface pressure-area ($\pi - A_m$) isotherm of 6CB,^[6,7] the surface area per molecule (A_m) was set to 37 Å²/molecule. Here 82 mesogen molecules were distributed at each side of the aqueous phase, with the -CN groups facing the aqueous phase as shown in Fig. 1(b). Hereinafter, we call this simulation system 'S82'. The MD simulation of S82 was carried out for 101 ns in the NVT ensemble using the NAMD software.^[14] The last 1 ns trajectory was used for analysis. The 6CB interaction parameters were taken from the OPLS-AA force field.^[15] All of the H-containing bonds are constrained with SHAKE. Periodic boundary conditions were considered in 3D space. The par-

**Corresponding author. Email: emine.cebe@ege.edu.tr
© 2018 Chinese Physical Society and IOP Publishing Ltd

ticle mesh Ewald summation technique^[16] was used to calculate the electrostatic interactions and long-range interactions were modeled by the Lennard-Jones potential, with a cutoff of 13 Å. Apart from the S82 system, we run another 41 ns MD simulation in the NVT ensemble at 297 K for the air-water-air (A/W/A) system with 5543 water molecules in the middle of the rectangular cell of size $54.984 \times 54.984 \times 300.000$ Å³. All codes used for the analysis of the simulation data were written by us. Images and graphs were produced using VMD^[17] and XMGRACE,^[18] respectively.

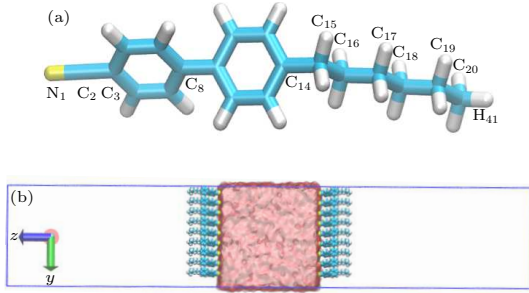


Fig. 1. (a) Schematic structure of 6CB with key atoms labeled. (b) A snapshot of the initial configuration of S82. Carbon, nitrogen and hydrogen atoms of 6CB are drawn in cyan, yellow and white, respectively. Water is rendered in transparent red.

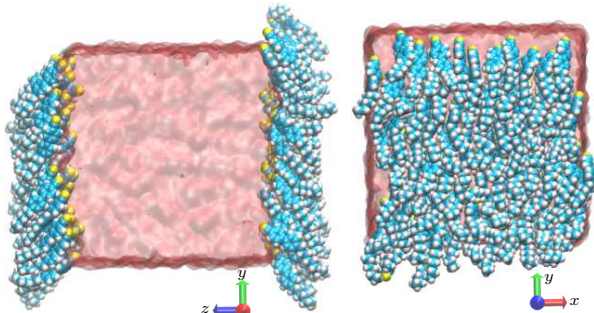


Fig. 2. Final snapshots (side and top view) of the simulated system. The color scheme for the snapshots is the same as Fig. 1.

It is clear from Fig. 2 that a monolayer occurs at the $A_m = 37$ Å²/molecule for S82. The cyano groups of 6CB molecules tend to penetrate to the A/W interface while the hydrophobic tails are mostly excluded from the water surface. The alkyl chains aggregate together and orient in a certain direction because of the interactions among them. The 6CB molecules exhibit a rough distribution producing a rippled surface at the A/W interface, contrasting to an almost flat interface at the beginning of the simulation (Fig. 1(b)).

The occurrence of monolayers can be seen from Fig. 3, depicting the mass density distributions of 6CB and water molecules. The mass density profiles of two monolayers are found symmetrically, indicating that the system is well equilibrated during the simulation. The presence of a ~ 55 Å thick water slab between two monolayers implies that the monolayer peaks are independent and have no influence on each other. The 6CB molecules are well adsorbed at the A/W interface

due to the strong interaction between the hydrophilic cyano groups and water molecules. The density of water in the bulk phase is 0.996 g/cm³ being in very good agreement with the experimental density of pure water, 0.997 g/cm³, which shows that the system under study is large enough.^[19] As seen from the snapshots and density profiles, the water molecules penetrate into the adsorption layer.

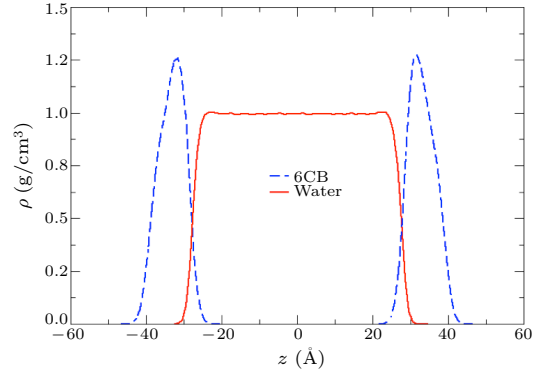


Fig. 3. Mass density profiles of the 6CB and water along the z axis.

To determine the interfacial thickness d , we fit the mass density profile of water to the usual hyperbolic tangent function given as

$$\rho(z) = \frac{1}{2}(\rho_L + \rho_V) - \frac{1}{2}(\rho_L - \rho_V) \tanh \left[\frac{(z - \delta)}{d} \right], \quad (1)$$

where ρ_L and ρ_V are the liquid and vapor densities, respectively, z is the distance along the normal to the interface, δ is the position of Gibbs's dividing surface and d is related to the 10–90 thickness being the distance between the z values at $0.9\rho_L$ and $0.1\rho_L$ by a factor of 2.1972. Table 1 gives the average liquid density and interfacial thickness of S82. We also performed the MD simulation of the interface between neat water and its vapor at 300 K and 1 atm, which gave $t = 3.7$ Å and $\rho_L = 0.996$ g/cm³. The reported thicknesses from simulations based on empirical polarizable water models are 3.2–3.9 Å.^[20–22] The roughness of the liquid-vapor interface for pure water obtained by x-ray reflectivity measurements is 3.2 Å.^[23] Comparing all these results with the thickness found in the current calculation (3.50 Å) implies that adding 82 molecules does not have a noticeable effect on the interface thickness.

Table 1. Fitted density profile parameters for water and 6CB at the liquid-vapor interface.

ρ_L (g/cm ³)	d (Å)	t (Å)	σ (Å)	z_0 (Å)
0.996	1.59	3.50	10.7	32.8

We calculated θ_{core} and θ_{tail} tilt angles, which quantify the orientations of the rigid cyanobiphenyl core and hydrocarbon chain vectors, respectively, relative to the interface normal. The corresponding results are listed in Table 2. The head and tail vectors are N_1 – C_{14} and C_{14} – H_{41} vectors, respectively (see Fig. 1(a) for atom labels). The adsorbed 6CB

molecules prefer a tilted orientation relative to the interface normal. The tilt angles calculated for the simulated system, namely 56.5° and 51.6° , are in good agreement with the experimental angles in the vicinity of the collapse point.^[6,7]

Table 2. Simulated tilt angles with respect to the normal interface, along with the experimental data.

θ_{core} (deg)	θ_{tail} (deg)	θ (deg) ^[6]	θ (deg) ^[7]
56.5	51.6	54	49

Table 3. The second and fourth rank orientational order parameters for rigid and alkyl parts of 6CB.

$\langle P_2 \rangle_{\text{rigid}}$	$\langle P_4 \rangle_{\text{rigid}}$	$\langle P_2 \rangle_{\text{alkyl}}$	$\langle P_4 \rangle_{\text{alkyl}}$
0.85	0.60	0.65	0.24

The mass density distributions of 6CB in Fig. 3 can be well-fitted with a Gaussian function

$$\rho(z) = \frac{A}{\sigma\sqrt{\pi/2}} e^{-4(z-z_0)^2/\sigma^2}, \quad (2)$$

where A is a constant, z_0 is the position of the peak center and σ is the monolayer width. The parameters that yielded the best fit are listed in Table 1. The monolayer width of 4'-*n*-octyl-4-cyanobiphenyl (8CB) in the liquid expanded phase was found to be 14 \AA by high-resolution x-ray reflectivity measurements at room temperature.^[24] Using the geometry of 6CB optimized by the DFT/RB3LYP/6-31G(d, p) approach, we computed the molecular length to be 20.3 \AA , which gives an approximate monolayer width of $\cos(56.5) * 20.3 = 11.2 \text{ \AA}$. These results are consistent with the current monolayer width of 10.7 \AA .

The second rank orientational order parameter $\langle P_2 \rangle$ was computed via the ordering matrix, whose elements are

$$Q_{\alpha\beta} = \frac{1}{2N_m} \sum_{j=1}^{N_m} (3u_{j\alpha}u_{j\beta} - \delta_{\alpha\beta}), \quad (3)$$

where $u_{j\alpha}$ are components of the long axis of molecule j , $\delta_{\alpha\beta}$ is the Kronecker δ symbol, and $\alpha, \beta = x, y, z$. The long molecular axis was found by diagonalizing the moment of inertia tensor. The largest eigenvalue and corresponding eigenvector of the order tensor are taken as $\langle P_2 \rangle$ and the phase director, respectively. We computed $\langle P_2 \rangle$ and the fourth rank order parameter (OP) given as

$$\langle P_4 \rangle = \langle (35 \cos^4 \theta - 30 \cos^2 \theta + 3)/8 \rangle, \quad (4)$$

where θ is the angle between the molecular long axis and director. For the rigid core, the simulated $\langle P_2 \rangle$ and $\langle P_4 \rangle$ values are 0.85 and 0.60, whereas the experimental ones for pure 6CB are ~ 0.6 and ~ 0.12 , respectively.^[25] The orientational order for interfacial systems increases considerably in comparison with that for pure nematic 6CB. The simulated OPs for the alkyl chain and rigid cyanobiphenyl core are listed in Table 3. The rigid core possesses higher OPs than those of the alkyl chain, as is expected.

The OPs for the CH alkyl segments were computed,

$$S_{\text{CH}} = \langle (3 \cos^2(\beta_{\text{CH}}) - 1)/2 \rangle, \quad (5)$$

where β_{CH} is the angle between the CH vector and the monolayer normal. As seen in Fig. 4, close to the aromatic ring region, hydrocarbon chains of 6CB become more ordered. The decrement of S_{CH} as the carbon atom number increases is due to the enhanced freedom of the carbons with the distance from the aromatic rigid part. Although the simulated and experimental results are qualitatively similar, the simulated OP for 6CB monolayer is higher suggesting more alignment than that indicated in the pure 6CB.^[26]

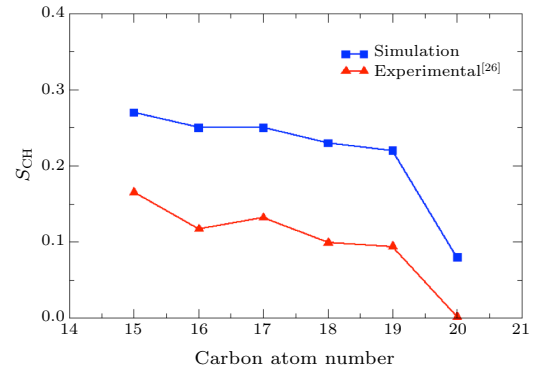


Fig. 4. Comparison of bond OPs for the hydrophobic tail with experimentally determined OPs of pure 6CB.^[26] The number of methyl carbon atoms of the chain is 20.

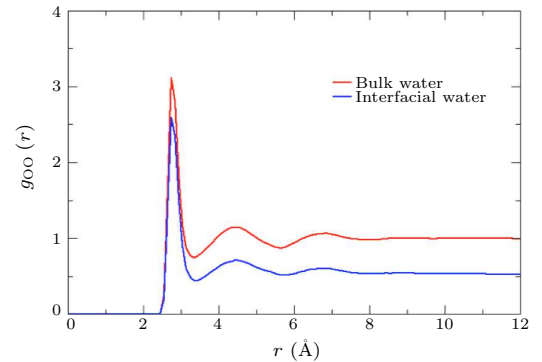


Fig. 5. The oxygen-oxygen RDFs for the bulk and interfacial water.

To study the local structure of water molecules in the bulk and interfacial regions, the oxygen-oxygen radial distribution functions (RDFs) were calculated. The bulk water region was taken between $z = \pm 2 \text{ \AA}$ and the interfacial water slab was considered to be the 10–90 thickness zone. Figure 5 shows the RDFs between oxygen atoms for two different water slabs. The previous TIP4P/2005 results and the corresponding RDF derived from the neutron diffraction for pure water are in agreement with those found in the current calculation for bulk phase.^[27,28] No change of the peak positions for both phases implies the almost unchanged local structure of water. The peak heights for the interfacial region are lower than those for the bulk

because of the decreasing number of water molecules in the interfacial region. The RDF in the interfacial region is converged to 0.5, as expected for a thin water slab centered on the Gibbs dividing surface.

To gain insights into the molecular interactions at the interfaces, we have calculated the distribution of hydrogen bonding between water molecules at the interface compared with those in the bulk water. In the following analyses, two water molecules are taken to be hydrogen bonded to each other if the distance of the water O atoms is less than 3.5 Å and simultaneously the angle of $O_{\text{acceptor}}-O_{\text{donor}}-H$ is less than 30°. The average number of hydrogen bonds per water molecule, n_{HB} , is found to be 3.5 in the bulk regions of S82 and A/W/A systems, compared with the experimental estimate for pure water (PW), $n_{\text{HB}}(\text{exp}) = 3.4$,^[29] being compatible with the tetrahedral picture of liquid water. This provides further

evidence for the similarity of bulk and pure water characteristics, as seen from the comparison of RDFs. Here n_{HB} decreases to ~ 2 for the interfacial regions because of the lower number density of water. In simulations of a number of water-organic liquid interfaces, this value varies from about 3.6 in the bulk about 2 at the interface.^[30]

The f_i fraction of water molecules having i hydrogen bonded neighbors in the interfacial and bulk water regions of both systems simulated has been calculated and is listed in Table 4. As is seen, the statistics for bulk regions are very close to those reported in Ref. [31] for pure water. The maximum of distributions shifts to smaller i values upon going from the bulk to the interfacial region. The bulk water molecules have three or four hydrogen bonded neighbors, whereas f_2 becomes the most populated fraction in the interface region.

Table 4. Fraction of the water molecules having i hydrogen bonded neighbors in the bulk and interfacial regions and in pure water, f_i (%). Here n_{HB} is the average number of hydrogen bonds per molecule.

i	S82		A/W/A		PW ^{a,c}	S82 ^b
	bulk ^a	surface ^a	bulk ^a	surface ^a		
1	2	28	2	25	1	90
2	10	44	10	43	7	9
3	30	26	30	29	29	0
4	52	2	51	3	56	0
5	6	0	6	0	7	0
n_{HB}	3.5	2.0	3.5	2.1	3.6	1.1

^aFor O...H-O hydrogen bonds, ^bFor N...H-O hydrogen bonds, ^cRef. [31].

It was reported that the main driving force of the adsorption is the possibility of forming hydrogen bonds between the adsorbed octyl cyanide and interfacial water molecules.^[32] Therefore, the calculated populations to characterize the hydrogen bonds formed by water and 6CB molecules are given in Table 4. We define 6CB and water molecules to be hydrogen bonded if their nitrogen-oxygen distances are less than 3.35 Å and simultaneously the nitrogen-hydrogen distance is less than 2.45 Å.^[32] The average number of hydrogen bonds per 6CB molecule and f_1 are found to be 1.1 and 91%, respectively, being in accordance with the fact that the $N \equiv C$ group can participate in only one hydrogen bond, being the H-acceptor partner.

We calculated the surface tension (γ), which was obtained from the pressure tensor,

$$\gamma = \left\langle \frac{L_z}{2} \left[P_{zz} - \frac{P_{xx} + P_{yy}}{2} \right] \right\rangle, \quad (6)$$

where P_{ii} ($i = x, y, z$) is the diagonal component of the pressure tensor, and L_z is the length of the simulation cell in the direction perpendicular to the air-water interface. The calculated surface tension of the A/W/A system is $\gamma_W = 67.8 \text{ mN/m}$, which agrees with the simulated and experimental results of 69.3 and 71.73 mN/m, respectively.^[33] The simulated surface tension of 90.1 mN/m for S82 is higher than that for the A/W/A system. For the slab coated with a monolayer, the surface tension of monolayer (γ_m) is computed as $\gamma - \gamma_W$. For the 6CB monolayer, γ_m is found to be 22.3 mN/m.

In conclusion, some morphological and structural features of 6CB monolayer at the A/W interface have been estimated for the first time by full atomistic MD simulations. The simulated mass density profiles and snapshots reveal the occurrence of stable monolayers. The simulated tilt angles for biphenyl core and alkyl parts, the interfacial thickness and monolayer width are consistent with the results reported previously. The second and fourth rank orientational OPs of 6CB, along with CH bond OPs, are computed. The orientational OPs for the interfacial system are much higher than those for pure nematic 6CB. It can be deduced from the calculated RDFs between oxygen atoms in bulk and interfacial water that adding 6CB molecules to the air-water interface does not change the local structure of water much. The surface tension calculations and hydrogen bond analysis are performed. The results are in good agreement with the experimental and simulation data.

We acknowledge TUBITAK ULAKBIM, the High Performance and Grid Computing Center (TR-Grid e-Infrastructure) for support with the computational sources.

References

- [1] MorenoRazo J A, Sambriski E J, Abbott N L, HernandezOrtiz J P and De Pablo J J 2012 *Nature* **485** 86
- [2] Fang J, Knobler C M and Yokoyama H 1997 *Physica A* **244** 91
- [3] Kaganer V M, Möhwald H and Dutta P 1999 *Rev. Mod.*

- Phys.* **71** 779
- [4] Daniel M F, Lettington O C and Small S M 1983 *Mol. Cryst. Liq. Cryst.* **96** 373
- [5] Zakharov A V and Iwamoto M 2002 *Phys. Rev. E* **66** 061605
- [6] Ingot K, Martyński T and Bauman D 2006 *Liq. Cryst.* **33** 855
- [7] Modlińska A, Ingot K, Martyński T, Dąbrowski R, Jadżyn J and Bauman D 2009 *Liq. Cryst.* **36** 197
- [8] Delabre U, Richard C and Cazabat A M 2009 *J. Phys.: Condens. Matter* **21** 464129
- [9] Jedlovsky P and Pártay L B 2007 *J. Mol. Liq.* **136** 249
- [10] RamezaniDakhel H, Sadati M, Rahimi M, RamirezHernandez A, Roux B and de Pablo J J 2017 *J. Chem. Theory Comput.* **13** 237
- [11] Gürbulak O and Cebe E 2017 *J. Dispersion Sci. Technol.* **110** (in press)
- [12] Abascal J L F and Vega C 2005 *J. Chem. Phys.* **123** 234505
- [13] Frisch M J et al 2009 *Gaussian 09 Revision A. 1 Gaussian, Inc.*
- [14] Phillips J C, Braun R, Wang W, Gumbart J, Tajkhorshid E et al 2005 *J. Comput. Chem.* **26** 1781
- [15] Jorgensen W L, Maxwell D S and TiradoRives J 1996 *J. Am. Chem. Soc.* **118** 11225
- [16] Darden T, York D and Pedersen L 1993 *J. Chem. Phys.* **98** 10089
- [17] Humphrey W, Dalke A and Schulten K 1996 *J. Mol. Graph.* **14** 33
- [18] Turner P 2005 *XMGRACE, Version 5. 1.19* (Center For Coastal and LandMargin Research, Oregon Graduate Institute of Science and Technology, Beaverton, Ore, USA)
- [19] Tanaka M, Girard G, Davis R, Peuto A and Bignell N 2001 *Metrologia* **38** 301
- [20] Kühne T D, Pascal T A, Kaxiras E and Jung Y 2011 *J. Phys. Chem. Lett.* **2** 105
- [21] Kuo I F W, Mundy C J, Eggimann B L, McGrath M J, Siepmann J I et al 2006 *J. Phys. Chem. B* **110** 3738
- [22] Wick C D, Kuo I F W, Mundy C J and Dang L X 2007 *J. Chem. Theory Comput.* **3** 2002
- [23] Braslau A, Deutsch M, Pershan P S, Weiss A H, AlsNielsen J and Bohr J 1985 *Phys. Rev. Lett.* **54** 114
- [24] Suresh K A, Shi Y, Bhattacharyya A and Kumar S 2001 *Mod. Phys. Lett. B* **15** 225
- [25] Kobinata S, Kobayashi T, Yoshida H, Chandani A D L and Maeda S 1986 *J. Mol. Struct.* **146** 373
- [26] Forster P and Fung B M 1988 *J. Chem. Soc. Faraday Trans. 2: Mol. and Chem. Phys.* **84** 1083
- [27] Vega C, Abascal J L F, Conde M M and Aragoes J L 2009 *Faraday Discuss.* **141** 251
- [28] Soper A K 2000 *Chem. Phys.* **258** 121
- [29] Pauling L 1960 *The Nature of the Chemical Bond* (Ithaca, New York: Cornell University Press) vol 260 p 3175
- [30] Michael D and Benjamin I 1998 *J. Electroanalytical Chem.* **450** 335
- [31] SwiatlaWojcik D 2007 *Chem. Phys.* **342** 260
- [32] Jedlovsky P and Pártay L B 2007 *J. Phys. Chem. B* **111** 5885
- [33] Vega C and de Miguel E 2007 *J. Chem. Phys.* **126** 154707